

Ivan Sulovsky\*, Zoran Čarija, Anton Turk, Jasna Prpić-Oršić

## Insights into high-fidelity propulsion modelling in ship hydrodynamics

University of Rijeka, Faculty of Engineering, Vukovarska 58, Rijeka, 51000, Croatia

\*Corresponding author: ivan.sulovsky@riteh.uniri.hr

Original scientific paper  
Received: January 26, 2026  
Accepted: April 27, 2026  
<https://doi.org/10.65776/ep.20.4.3>



### Abstract

*This paper presents a Coupled Sliding Mesh (CSM) propulsion model for high-fidelity ship hydrodynamics simulations implemented within OpenFOAM. The model integrates rigid body motion with propeller rotation using Arbitrary Mesh Interface and morphing mesh approach. The model is validated against experimental data from self-propulsion tests on the Duisburg Test Case hull model at SINTEF, Norway, including calm water and three regular head wave cases. Grid comparative assessment demonstrated accurate capture of the self-propulsion point, with resistance deviating less than 1% from propeller thrust. Frequency domain analysis revealed successful capture of characteristic frequencies: wave encounter frequency, first shaft harmonic, and blade passing frequency. This study demonstrates that high-fidelity propulsion assessments can be achieved using open-source CFD tools for complex propeller-hull interaction problems.*

**Keywords:** ship hydrodynamics, propeller modelling, OpenFOAM, CFD, self-propulsion

### 1. Introduction

Computer power and numerical tools for ship hydrodynamics have developed rapidly in recent years. As a result, evaluating ship propulsion performance has shifted from traditional experimental testing toward computational approaches. Towing tanks, however, remain an indispensable asset that complements these computational tools. Among the available numerical methods, Computational Fluid Dynamics (CFD) based on Reynolds-averaging has become the dominant approach for solving a wide range of problems in ship hydrodynamics.

This paper addresses the modeling of propeller effects using a high-fidelity approach within the OpenFOAM toolbox [1]. OpenFOAM is an open-source CFD software based on a second-order collocated Finite Volume (FV) method. It has gained wide acceptance in research and academia due to its flexibility, allowing for extensive customization and user-developed improvements. Regarding the specific CFD modelling of the propeller effects, it is necessary to outline the most common methods used. The most straightforward approach represents propeller thrust and torque through virtual forces, eliminating the need to explicitly model the propeller geometry. These techniques fall under *body force* methods, alternatively referred to as actuator disk or virtual disk approaches. The core principle involves distributing forces within the propeller zone in a manner that remains consistent across different propeller designs. This consistency in force distribution was first examined nearly a century ago and given in [2], where findings continue to serve to this day for the body force group of methods.

The application of such propeller model has been successfully validated across many codes [3,4,5]. Since the main aim of this paper lies in a fully discretized propeller model in contrast to simplified body force method, an extensive

review of the body force methods application is omitted. The most notable disadvantage of the body force methods is their inability to capture local flow features both upstream and downstream of the propeller plane. This is however compensated with high computational efficiency. A second group of methods for modelling propeller effects is based on a complete representation of propeller geometry with direct modelling of the rotation. Within the FV framework, propeller rotation can be modelled using overset technology [6,7] or via Arbitrary Mesh Interface (AMI) [8]. Also, a Moving Reference Frame (MRF) method is often applied in order to initialize the solution of the flow around the propeller [9,10].

In this paper, a novel numerical propulsion model is outlined that has been implemented in OpenFOAM code. The model is based on coupling motions between rigid body motion of the hull and a priori known rotating motion of the propeller, while using the advantages of both AMI interface and morphing mesh approach. The model is tagged with an acronym Coupled Sliding Mesh (CSM). Brief outline of the mathematical model of fluid flow is given in Section 2. In Section 3, experimental data with corresponding setup on the DTC hull model, originating from SINTEF, Norway is given. This is followed with a more detailed description of the CSM numerical propulsion model in Section 4. In Section 5, results of the self-propulsion tests in calm water and waves with propeller being modelled using CSM approach is given with a focus on the torque frequency content. While the CSM model and time-averaged self-propulsion results for the DTC hull have been previously reported by the authors [14], the present work extends that study through a systematic frequency-domain analysis of the propeller torque signal, identifying shaft harmonics and blade passing frequency components under calm water and regular head wave conditions. Lastly, conclusions and future work are outlined.

## 2. Mathematical model of fluid flow

In this Section, a mathematical model of fluid flow is given. Fluid flow is governed by Navier-Stokes (NS) equations for incompressible flows, the continuity equation (1) and momentum equation (2):

$$\nabla \cdot \mathbf{u} = 0 \quad (1)$$

$$\frac{\partial \mathbf{u}}{\partial t} + (\mathbf{u} \cdot \nabla) \mathbf{u} - \nu \nabla^2 \mathbf{u} = -\frac{1}{\rho} \nabla p + \mathbf{g} \quad (2)$$

where  $\mathbf{u}$  represents the local fluid velocity. The left-hand side of the Navier-Stokes equation comprises three components: The total derivative representing temporal velocity changes, the convective transport term, and the viscous diffusion term. The term denotes the pressure gradient,  $\mathbf{g}$  represents gravitational acceleration, and indicates the effective kinematic viscosity. To solve these governing equations, a multi-phase solver is employed, designed for two incompressible, isothermal, immiscible fluid phases (water and air). The air-water interface is captured using the Volume of Fluid (VOF) methodology, which introduces an indicator function  $\alpha$  into the governing equations. This scalar field  $\alpha$  modifies the Navier-Stokes equations by affecting the density  $\rho$  and effective kinematic viscosity, as shown in equations (3) and (4), respectively.

$$\rho = (1 - \alpha)\rho_{air} + \alpha\rho_{water} \quad (3)$$

$$\nu = (1 - \alpha)\nu_{air} + \alpha\nu_{water} \quad (4)$$

For accurate interface capturing, *isoAdvector* scheme is used [11]. The temporal discretization employs a first-order temporal scheme for calm water simulations while a second-order accurate backward scheme is set for transient simulations in waves. Convective fluxes are discretized using a linear scheme that transitions to an upwind-biased approach in regions with strong gradients, following the local flow direction. Diffusive gradient terms utilize Gaussian linear interpolation for their discretization. The pressure-velocity coupling is handled through the PIMPLE algorithm, configured with four iterations per time step: two dedicated to pressure residual reduction and two for the momentum equation solution.

Hydrodynamic coupling between the rigid body motion of the ship and the surrounding fluid is achieved using a six-degree-of-freedom solver, with constraints applied to the surge, sway, yaw, and roll motions. Mathematical closure of the Navier-Stokes equations, i.e., resolving turbulent fluxes, within the Reynolds-averaging concept is achieved using  $k-\omega$  SST model. Regarding linear solvers, for solving large sparse matrices that are yielded from a FV mesh, a conjugate gradient (CG) method is chosen with a Cholesky preconditioner. Residual tolerance is

set to  $1^{-6}$ . Velocity components and turbulence terms are solved using a smooth solver, i.e., Gauss–Seidel smoother with a residual tolerance of  $1^{-8}$ . With depiction of linear solvers this Section is concluded. Next Section outlines experimental data on the Duisburg Test Case (DTC) hull model in both calm water and regular head waves.

## 3. Experimental data

In this Section, experimental data using the DTC hull model, originally developed in [12] is presented. A comprehensive series of model tests was conducted at SINTEF in Trondheim, Norway, one of Europe's largest independent research institutions. Complete experimental procedures are documented in [13,14]. Rigid body motion tracking is performed using an Oqus optical positioning system, while propeller thrust and torque are recorded via a dynamometer. The reflective markers required for optical tracking, along with the umbilical cable supplying power and enabling data transmission, are visible in Figure 1.

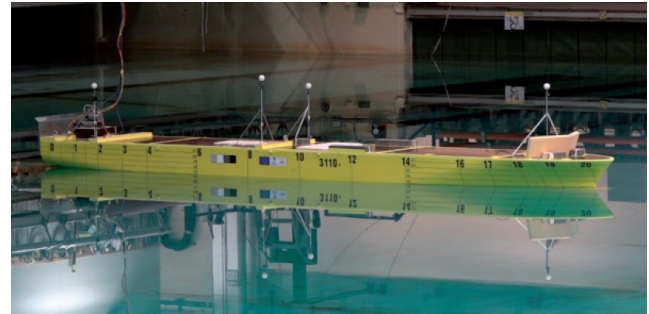


Fig. 1. DTC model. Reprinted with permission of the author [13,14]

Constructed at 1:63.65 scale, the model features a five-bladed fixed-pitch propeller and a twisted rudder equipped with a costa bulb. Rather than being towed, the ship operates in free-running mode, employing an autopilot system. Main particulars along with inertial characteristics of the model are shown in Table 1.

Main Parameter	Value
Scale, $\lambda$	63.65
Length between perpendiculars $L_{pp}$ , m	5.577
Breadth $B$ , m	0.801
Draught $T$ , m	0.228
Displacement, $\Delta$ , kg	672.6
Pitch moment of inertia, $I_{55}$ kgm <sup>2</sup>	1266.3
Long. center of gravity, $LCG$ , m	2.721

Table 1. DTC main parameters.

Self-propulsion test in calm water is performed at a propeller revolution rate of 11.5 rps with achieved speed of 1.03 m/s. Experiments in waves are performed at the same propeller revolution rate, under wave conditions listed in Table 2.

Wave case	1 <sup>st</sup>	2 <sup>nd</sup>	3 <sup>rd</sup>
Wave height, $H$ , m	0.06	0.087	0.119
Wave period, $T$ , s	0.82	1.24	1.49
$H/L_{pp}$ -	0.011	0.0157	0.02
$\lambda_c/L_{pp}$ -	0.187	0.303	0.46

**Table 2.** Experimental conditions of self-propulsion tests in waves

Next Section deals with a numerical model developed within OpenFOAM framework with its main intention of enabling high-fidelity propulsion assessments.

#### 4. Coupled Sliding Mesh (CSM) model

This Section describes the coupled sliding mesh model for hydrodynamic simulations utilizing both rigid body motions with propeller rotation. The new functionality is implemented in the existing OpenFOAM class that computes fluid-induced rigid body responses in CFD simulations. The main novelty in the CSM model is the coupled propeller rotation with rigid body motion, utilizing the usage of both AMI and morphing mesh. The main motivation for this numerical model is to avoid using overset mesh methodology which is based on volumetric interpolations of fields, opposing to the face-based interpolations that sliding mesh offers. A discretized propeller in the stern of the DTC model is shown in Figure 2.

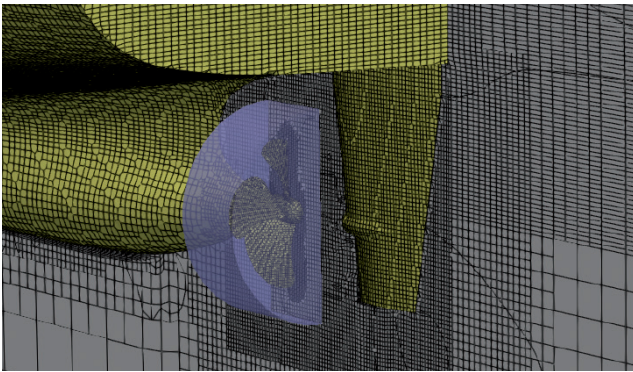


**Fig. 2.** Typical mesh topology for CSM model

Volumetric interpolations, as indicated in [15], are highly sensitive to the chosen interpolation procedure. Low-order interpolation scheme seem to cause mass imbalances within the domain which can have profound effects on the accuracy and validity of the simulations. High-order schemes perform slightly better, producing smoother fields, but are still prone to errors. Also, using overset mesh will inherently require significantly higher cell count. The usage of overset methodology is in some sense required when the geometries are complex and AMI interfaces are difficult to obtain. The main limitation of the model is that it does not overcome the well-known computational requirements necessary for any fully-resolving rotating geometries in CFD where the time step is dictated by the angle increment of the propeller within one

iteration. This increment is usually of the order of  $1^\circ$ - $5^\circ$ , depending on the propeller rate of revolution. The computational workflow of the algorithm is given in Figure 3.

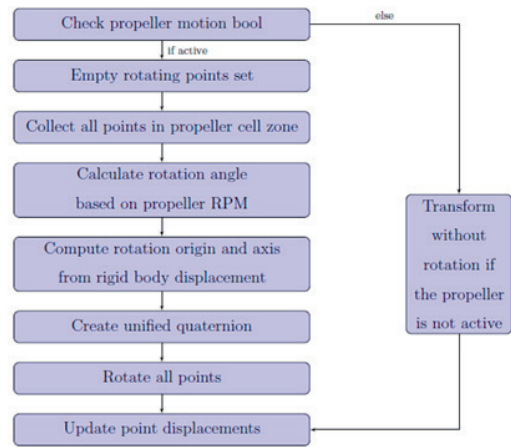


**Fig. 3.** Computational workflow of the CSM class

For the detailed description of the computational workflow and modifications to the existing OpenFOAM classes the interested reader is referred to [16].

#### 5. Results and discussion

The results presented in this Section are partly given in author's previous work, presented in [17]. However, in this study, frequency content of the torque signal exhibited from the CSM model are explored further. In order to quantify the discretization errors, self-propulsion test in calm water is conducted on two grid sizes. The traditional grid sensitivity study is omitted due to high computational load of the simulations. In Figure 4, discretized stern region of the DTC hull along with the entire computational domain shown in Figure 5. The computational domain extends 1 ship lengths upstream, 3 lengths downstream, and 1 lengths in the transverse and vertical directions. The time-step size is set to 1 ms, corresponding to a propeller rotation increment of approximately  $4^\circ$  per time step. The inlet and outlet boundary conditions account for active wave generation [18]. For the frequency domain analysis, a DFT is applied over a window that corresponds to the wave encounter period using Hann window function.

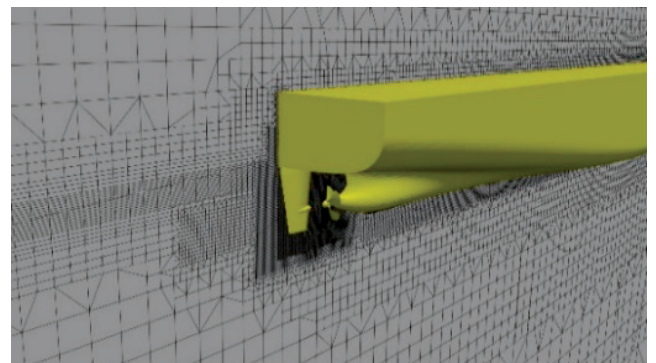


**Fig. 4.** Stern region of the DTC hull

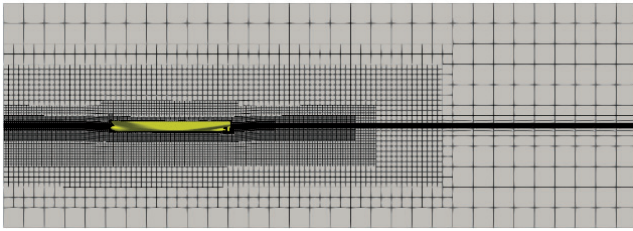


Fig. 5. Computational domain in transverse view

The results of the self-propulsion test in calm water, conducted on two grid sizes is given in Table 3. The coarse grid contains approximately 5.6 million cells and the fine grid 9.8 million cells. The refinement is applied uniformly with an approximate ratio of . The boundary layer is discretized in order to yield a non-dimensional distance commonly known as  $y^+$  around 30 for the flow around the hull while more stringent discretization is placed upon the propeller blades in order to achieve a value of 5.

	Experiment	Coarse grid	Fine grid
Thrust, $T$ , N	14.126	14.965	14.321
Torque, $Q$ , Nm	0.323	0.327	0.311

Table 3. Results of the self-propulsion test

It is important to emphasize that the self-propulsion point is correctly captured. The total resistance in both coarse and fine grid deviated no more than 1% compared to the propeller thrust. The swirling flow exhibited from the propeller motion, with colour scale showing the dimensionless flow speed is given in Figure 6

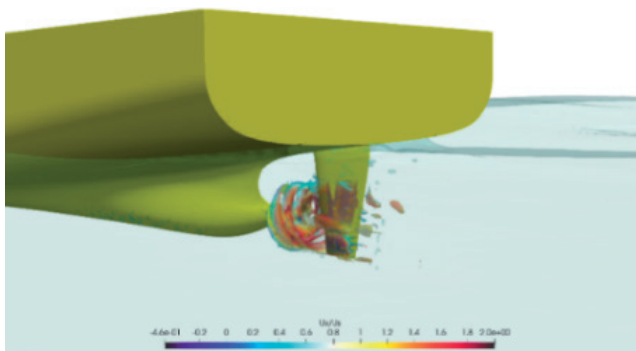


Fig. 6. Flow structures behind propeller

The comprehensive results of the self-propulsion in waves along with propeller-hull interactions are given in [19]. Instead, the focus of showcasing the results of self-propulsion tests is the frequency content that is embedded in torque signals of the propeller. The frequency content observed in the time domain signal of the propeller torque can be directly related to the propeller rotational characteristics [19,20]. For a propeller with  $N$  blades rotating at  $f_{rot}$ , the Blade Passing Frequency can be formulated as:

In the present case of the DTC hull operating with a five-bladed propeller at a frequency of 11.5 rps (Hz), the resulting BPF occurs at 57.5 Hz. In addition, shaft harmonics occur at integer multiples of the rotation frequency  $f_{rot}$ , formulated simply as:

Shaft harmonics are associated with non-uniform inflow and unsteady loading of the propeller in behind-hull conditions. The frequency content of the torque signal computed by CFD and experiment, across all three wave cases are given in Figures. 7., 8., and 9. respectively. The conversion from time to frequency domain has been done using Discrete Fourier Transform (DFT) method.

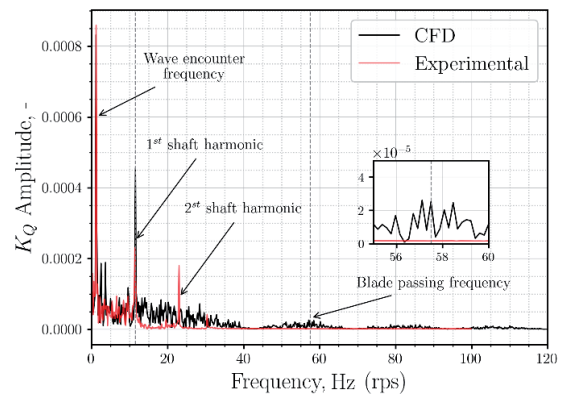


Fig. 7. Frequency content of the torque signal for the 1<sup>st</sup> wave case

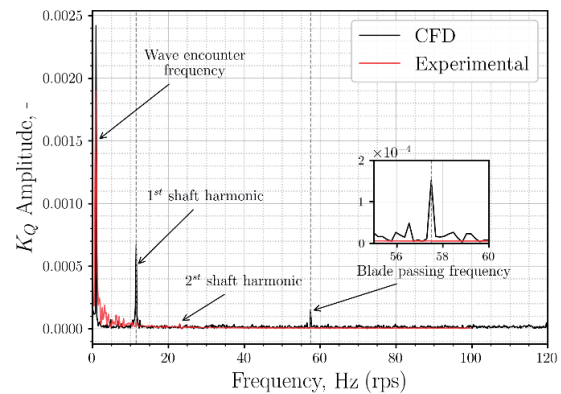


Fig. 8. Frequency content of the torque signal for the 2<sup>nd</sup> wave case

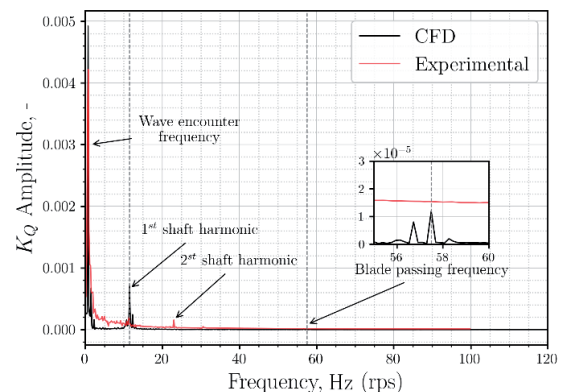


Fig. 9. Frequency content of the torque signal for the 3<sup>rd</sup> wave case

The frequency domain analysis of the propeller torque provides additional insight into the unsteady loading mechanisms acting on the propeller in waves, which cannot be fully assessed from time-averaged quantities alone. For all three wave cases, the dominant low-frequency peak corresponds to the wave encounter frequency, indicating that the propeller loading is strongly modulated by the incoming wave system. Across all cases, distinct peaks are observed at the first and second shaft harmonics, as well as at the blade-passing frequency. However, 2<sup>nd</sup> shaft harmonic is consistently captured in the experiment while only a slight peak from the CFD results is observed for case 2, Figure 7. This might be attributed to numerical noise or general polyhedral mesh discretization. The Blade Passing Frequency at 57.5 Hz occurs consistently in CFD computations for every case while it is not captured by the dynamometer in the experiments. Higher harmonics of the blade passing frequency were not captured both in CFD and experiments. While the dominant frequency peaks are correctly identified by the CFD model, amplitude discrepancies at higher frequencies, particularly beyond the first shaft harmonic are attributed to the current grid resolution and are considered acceptable given the simplified grid sensitivity that is performed.

These frequency components show that the CFD model captures both the large-scale unsteadiness from ship motion and wake non-uniformity, along with the high-frequency local blade loading effects. The CFD and experimental results agree well in identifying these characteristic frequencies, indicating that the main physical mechanisms are correctly represented. However, amplitude differences appear, particularly at higher frequencies. It is important to emphasize that the spatial discretization of the propeller blades has a significant impact on the exerted forces. In this study, an open-source tool *snappyHexMesh* is used, that is based on designing robust body-fitted polyhedral mesh around arbitrary geometries. For discretizing the propeller, strictly polyhedral cell type is not an ideal discretization approach, since it can produce artificially rough surface due to its polyhedral algorithm. The consequence of having polyhedral cells around the propeller blade can result in additional numerical noise due to summation of forces on cells that can exhibit significantly different face normals [21]. The advantages of block-structured mesh in reducing such numerical artifacts have been well documented [22], though their generation for complex propeller geometries remains a challenge. Nevertheless, in this work it is shown that even with open-source tools, a high-fidelity result can be yielded in complex propulsion assessment in ship hydrodynamics.

## 6. Conclusions

This paper presented a novel Coupled Sliding Mesh (CSM) propulsion model implemented within the OpenFOAM framework for high-fidelity ship hydrodynamics simulations. The model couples rigid body motion of the hull with propeller rotation using Arbitrary Mesh Interface (AMI) technology and morphing mesh approach, avoiding the volumetric interpolations inherent to overset methodologies that can introduce mass imbalances and

require higher cell counts. The CSM model was validated against experimental data from self-propulsion tests on the DTC hull model conducted at SINTEF, Norway, covering both calm water and three regular wave cases. Grid comparative analysis on two mesh resolutions demonstrated that the self-propulsion point was correctly captured, with total resistance deviating no more than 1% from propeller thrust in both coarse and fine grids.

Frequency domain analysis of propeller torque signals revealed that the CSM model successfully captures the characteristic frequencies associated with propeller-hull interactions. For all wave cases, the dominant low-frequency peak corresponding to the wave encounter frequency was observed, indicating strong modulation of propeller loading by the wave system. The first shaft harmonic and blade passing frequency at 57.5 Hz were consistently captured in CFD results, demonstrating that the model correctly represents both large-scale unsteadiness from ship motion and high-frequency local blade loading effects. However, the second shaft harmonic and higher harmonics of the blade passing frequency showed weaker agreement with experiments, likely attributed to numerical noise, DFT parameters, and limitations of the polyhedral mesh discretization around propeller blades using *snappyHexMesh*. Despite these limitations, the study demonstrates that high-fidelity propulsion assessments in ship hydrodynamics can be achieved using open-source tools and the CSM approach, providing a viable alternative to overset methodologies for complex propeller-hull interaction problems.

## Acknowledgments

This work was supported by the Croatian Science Foundation under the project HRZZ-IP-2022-10-2821.

This work was also supported by the University of Rijeka (PROJECTS no. PU-17 uniri-iz-25-10 - Funded by the European Union – NextGenerationEU).

## References

- [1] Weller, H.G., Tabor, G., Jasak, H., and Fureby, C. A tensorial approach to computational continuum mechanics using object-oriented techniques. *Computer in Physics*, 12(6):620–631, 11 1998. ISSN 0894-1866. doi:10.1063/1.168744
- [2] M. E. Goldstein. On the optimum velocity distribution for a propeller in axial flow. *Journal of the Aeronautical Sciences*, 2:1–12, 1929.
- [3] Wang, H., Xiang, X., Xiang, G., Liu, C., Lichun and Yang, L. An improved body force method for simulation of self-propulsion auv with ducted propeller. *Ocean Engineering*, 281:114731, 2023. ISSN 0029-8018. doi: 10.1016/j.oceaneng.2023.114731
- [4] Sulovsky, I., Mewes, S., El Moctar, O., and Prpić-Oršić, J. CFD study on a full-scale ship performance in a representative sea state. *Ocean Engineering*, 333:121519, 2025. ISSN 0029-8018, doi: 10.1016/j.oceaneng.2025.121519
- [5] Yu, J., Yao, C., Liu, L. Application of virtual disk propulsion model for self-propelled surface ship in regular head wave. *Journal of Marine Science and Technology*, 28:471–495, 2023. doi: 10.1007/s00773-023-00935-8.

- [6] Đurasević, S., Gatin, I., Uroić, T., and Jasak, H. Hydrodynamic performance of a full-scale ship with a pre-swirl duct: A numerical study with partially rotating grid method. *Ocean Engineering*, 283:115049, doi:10.1016/j.oceaneng.2023.115049
- [7] Omar, N., Yoshiki, M., Yusuke, A., Sano, M., Hosogaya, K., and Maki, A. CFD based study on interaction between VecTwin rudders, propeller and hull during stopping maneuver and around hover region, *Ocean Engineering*, Volume 342, Part 1, 2025, ISSN 0029-8018, doi:10/1016/j.oceaneng.2025.122828
- [8] P.E. Farrell, P.E. and Maddison, J.R. Conservative interpolation between volume meshes by local galerkin projection. *Computer Methods in Applied Mechanics and Engineering*, 200(1):89–100, 2011. ISSN 0045- 7825. doi: 10.1016/j.cma.2010.07.015.
- [9] Ye, Z., Su, S., Zhou, L., Liu, Z. and Luo, X: Numerical study of water depth effects on the hydrodynamic performance of a shallow-water seismic survey ship's Z-drive ducted propeller. *Brodogradnja 76 (4) (2025) 76401*
- [10] Kiss-Nagy, K. and Simongati, G. Digital twin of USV thruster based on CFD simulations and towing tank experiments. *Brodogradnja 76 (4) (2025) 76403*
- [11] Roenby, J., Bredmose, H., and Jasak, H. A computational method for sharp interface advection. *Royal Society Open Science*, 3:160405, 2016.
- [12] Shigunov, V., el Moctar, O. and Zorn, T. Duisburg test case: Post-panamax container ship for benchmarking. *Ship Technology Research*, 59(3):50–64, 2012. doi: 10.1179/str.2012.59.3.004.
- [13] Øyvind Rabliås. *Numerical and Experimental Studies of Maneuvering in Regular and Irregular Waves*. PhD thesis, NTNU, Trondheim, 2022.
- [14] Øyvind Rabliås, Ø. and Trygve, K. A rational model for maneuvering in irregular waves with the effect of waves on the propeller and rudder inflow taken into account. *Ocean Engineering*, 243:110186, 2022. ISSN 0029-8018, doi: 10./1016/j.oceaneng.2021.110186
- [15] Lemaire, S., Vaz, G., van Rijswijk, and Turnock, S.R. Influence of Interpolation Scheme on the Accuracy of Overset Method for Computing Rudder-Propeller Interaction. *Journal of Verification, Validation and Uncertainty Quantification*, 8(1):011002, March 2023. doi: 10.1115/1.4056681.
- [16] Sulovsky, Ivan. *Numerical modelling of ship propulsion characteristics in sea waves: doctoral thesis*. Diss. Sveučilište u Rijeci, Sveučilište u Rijeci-Tehnički fakultet, Zavod za brodogradnju i inženjerstvo morske tehnologije, 2026.
- [17] Sulovsky, I., Bakica, A. and Prpić-Oršić, J: CFD assessment of ship propulsion and propeller-hull interactions in waves using low and high fidelity approach. *Ocean Engineering*, 346:123843, 2026. ISSN 0029-8018. doi: 10/1016/j.oceaneng.2025.123843
- [18] Higuera, P., et al., 2013. Realistic wave generation and active wave absorption for navier-Stokes models: application to openFOAM®. *Coastal Eng.* 71, 102–118. <https://doi.org/10.1016/j.coastaleng.2012.07.002>
- [19] Witte, M., Nolte, N., Hinnenhal J. and Wurm, F.H. Hydroacoustic investigations of a marine propeller based on holography. *Ocean Engineering*, 345:123231,2026, ISSN:0029-8018. doi:10.1016/j.oceaneng.2025.123231
- [20] Ebrahimi, A., Seif, M.S., Nouri-Borujerdi, A. Hydrodynamic and Acoustic Performance Analysis of Marine Propellers by Combination of Panel Method and FW-H Equations. *Math. Comput. Appl.* 2019, 24, 81. <https://doi.org/10.3390/mca24030081>
- [21] Bakica, A., Vladimir, N. and Koričan, M. Propeller retrofit on a fishing vessel: Self-propulsion CFD simulations with existing and new propeller. *Sustainable Development and Innovations in Marine Technologies*. 2025
- [22] Sikirica, A. Čarija, Z. Kranjčević, L. and Lučin, I. Grid Type and Turbulence Model influence on Propeller Characteristics Prediction. *J. Mar. Sci. Eng.* 2019, 7, 374.